IEEE Access
Multidisciplinary | Rapid Review | Open Access Journal

Received May 19, 2019, accepted May 31, 2019, date of publication June 5, 2019, date of current version June 19, 2019.

Digital Object Identifier 10.1109/ACCESS.2019.2920989

Sensitivity Analysis and Optimal Design of a Linear Magnetic Gear for Direct-Drive Wave Energy Conversion

CHUNYUAN LIU[1], HE ZHU[1], RUI DONG[1], SHIGUI ZHOU[2], AND LEI HUANG[3], (Member, IEEE)

[1]College of Mechanical and Electrical Engineering, Jiaxing University, Jiaxing 314000, China
[2]School of Engineering, Qufu Normal University, Rizhao 276826, China
[3]School of Electrical Engineering, Southeast University, Nanjing, China

Corresponding author: Chunyuan Liu (liuchunyuan_zjx@163.com)

This work was supported in part by the Natural Science Foundation of China, under Grant 41876096, in part by the Zhejiang Provincial Natural Science Foundation of China, under Grant LY19E070004 and Grant LY17E070006, in part by the Natural Science Foundation of Shandong Province, under Grant ZR2014EEM013, and in part by the project of Jiaxing Science & Technology bureau China, under Grant 2017AY13017.

ABSTRACT An optimized method for the linear magnetic gear (LMG) is proposed in the present study and the designed LMG is employed in the direct-drive wave power generation system. Conventional methods, such as analytical methods, may be inapplicable. Unlike the conventional motor structures, the proposed LMG has the double air-gap structure, which makes it more difficult for the design optimization. Therefore, a practical and effective method that combines the finite element analysis (FEA) and particle swarm optimization (PSO) is proposed to optimize the LMG. In order to decrease the computational expense of the optimization, main factors are categorized, based the influence on the motor performance. They are categorized into sensitive and non-sensitive parameters in this regard. Then, the FEA–PSO method is used to optimize sensitive parameters. The lower-speed and higher-speed parts of the optimized LMG are connected to the buoy and the secondary parts of the permanent magnet linear generator (PMLG), respectively, so that the wave energy converter is employed in the direct-drive wave power generator system. The present study shows that the proposed LMG method can be applied to adjust the frequency of the secondary motor, equal to or close to the natural frequency of the seawater. Therefore, the proposed method can be employed to obtain the maximum wave power. In order to validate the performance of the optimal design, a prototype is produced and tests are carried out.

INDEX TERMS Linear magnetic gear (LMG), finite-element method (FEM), field flux modulation, optimal design.

I. INTRODUCTION

With the development of economy and society, the annual increment of the energy demand is inevitable. On the other hand, limitations in fossil fuels make renewable energy resources more important. Wave energy is one of renewable energies, which has a huge storage in oceans. Researches show that controlling only 0.2% of the ocean's untapped energy is sufficient for the energy consumption of the entire world. Therefore, the wave energy is of significant importance, from this point of view. The wave energy is an important type of renewable energy so that the development and utilization of the wave energy is highly demanded. Many scholars have done variety of researches on how to effectively use the wave energy. Especially in areas, where the wave energy is abundant and other energy resources are scarce, harnessing the wave energy is of great importance to the social and economic development.

There are different methods to harness the wave energy, such as oscillating water column (OWC) [1]–[3] and the overtopping [4], [5] systems. Most of these methods employ rotating electrical machines to transform the kinetic energy of waves into the electrical energy. In these methods, the wave energy is converted to the mechanical energy and then, it is converted to the electrical energy. These sequential

The associate editor coordinating the review of this manuscript and approving it for publication was Sotirios Goudos.

2169-3536 © 2019 IEEE. Translations and content mining are permitted for academic research only.
Personal use is also permitted, but republication/redistribution requires IEEE permission.
See http://www.ieee.org/publications_standards/publications/rights/index.html for more information.

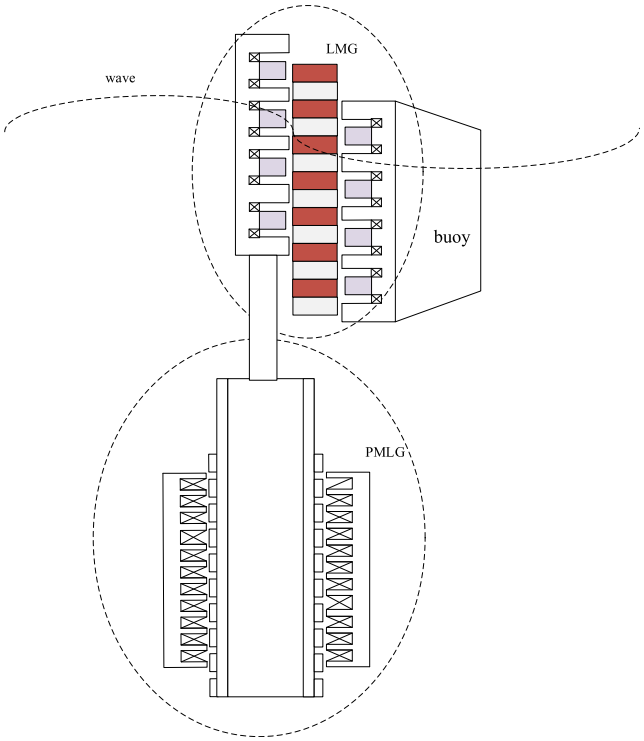

FIGURE 1. The schematic diagram of the wave power take-off system.

conversions lead to low overall efficiency and low safety performance of the methods. Moreover, both methods require high installation sites with complex installation procedures. Another system for employing the wave energy is the direct-drive wave energy converter method, including ocean power technologies (OPT) [6]–[8] and Archimedes wave swing (AWS) [9]–[11] methods. These methods eliminate the intermediate conversion devices and directly use the buoy, which has the oscillatory up and down motion with waves to drive the permanent magnet linear generator (PMLG). This method has lower installation and maintenance costs, while it noticeably improves the overall efficiency and reliability of the system. However, the linear generators for direct-drive wave energy converters always run at low and reduced conversion efficiencies. Therefore, the challenge for the wave power generator systems, is finding a way to increase the movement velocity of the linear generator. Based on the above considerations, the present work proposes a high speed direct-drive wave power take-off system. Fig. 1 illustrates the schematic diagram of the proposed system. It indicates that the system consists of the LMG, PMLG and the buoy. The buoy is rigidly connected to the low-speed mover of the LMG, and it fluctuates in accordance with the wave motion. While the high-speed mover is also rigidly connecteded to the primary part of the PMLG this structure can improve the stability and security of the system. The speed of PMLG is increased according to the principle of magnetic field modulation, where the speed of the direct-drive wave power take-off system increases under the action of the LMG. Therefore, the power generation efficiency of the system improves.

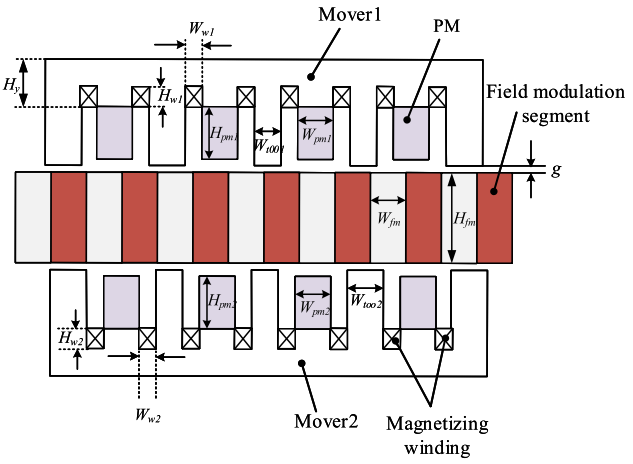

FIGURE 2. Linear magnetic gear and design parameter model.

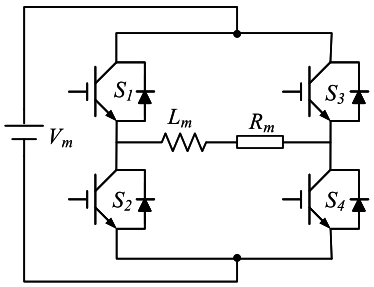

FIGURE 3. Magnetizing/demagnetizing DC circuit.

II. CONFIGUARTION OF THE LMG

A. LMG CONFIGURATION

Fig. 2 illustrates the configuration of LMG. It indicates that the LGM is composed of the two movers and a field modulation segment. Moreover, the mover consists of a permanent magnet, magnetizing windings and back iron. Permanent magnet is made of AlNiCo material and has low coercivity. Magnetic characteristics of the permanent magnet can be adjusted through introducing electric pulses to the magnetizing winding. Each PM pole has a pair of windings, which is used for magnetizing and demagnetizing. Stationary field modulation segments are located in the middle of two movers. Since there is no need to detect the mover position, the proposed structure brings great convenience to control algorithm. The magnetizing/demagnetizing DC circuit is shown in Fig. 3. an H-bridge circuit is used for driving each magnetizing winding, where L_m and R_m are the inductance and resistance of a magnetizing coil, respectively. This H-bridge circuit can control the current amplitude and direction for magnetizing/demagnetizing AlNiCo PMs.

B. WORKING PRINCIPLE OF THE LMG

The low-speed mover moves a distance, while the high-speed mover moves a larger distance under the influence of magnetic gear. All permanent magnets participate in force transmission during the force transmission process, which can

effectively improve the utilization rate of permanent magnets. Researchers proved that this novel magnetic gear structure can overcome the shortcomings of the small transmission force for conventional permanent magnet gear transmissions and has the same transmission capacity as those for mechanical gears [12].

The field modulation segment is designed to set the inner and outer permanent magnets so that it can modulate the magnetic field of the LMG. Based on the principle of magnetic field modulation, the field modulation segment pole-pair number Q, the pole-pair number of PMs n_1 and n_2 should satisfy the following mathematical relationship:

$$n_2 = |Q \pm n_1| \tag{1}$$

Moreover, the gear ratio G_r is governed by:

$$G_r = \frac{v_h}{v_l} = \frac{n_2}{n_1} \tag{2}$$

where v_h and v_l denote the high and low mover speed, respectively. Furthermore, for the space harmonic field distribution, pole pair numbers can be calculated as the following:

$$p_h = |mp + kn_s| \tag{3}$$

where $m = 1, 3, 5 \ldots, k = 0, \pm1, \pm2, \ldots, i = 0$ indicates that there is no field modulation segment. p is the pole-pair number of PM for the high-speed and low-speed mover.

The space harmonic linear velocity of the air gap magnetic field is given by:

$$v_{m,k} = \frac{mp_h}{mp_h + kn_s} v_r + \frac{kn_s}{mp_h + kn_s} v_s \tag{4}$$

where v_s, v_r are the linear velocities of the field modulation segment and the PM, respectively.

The transmission ratio of the linear magnetic gear can be obtained from equations (1)-(4). It should be indicated that, when discussing the harmonic pole-pair number of a magnetic field, there are only two cases to consider:

1) $k = 0$, when there is no field modulation segment and there is no magnetic field modulation effect.

2) $m = 1$, $k = -1$, when the largest space harmonic component, except for the fundamental harmonic is obtained. For this case, equation (2) can be re-written as:

$$v_{1,-1} = \frac{p_h}{p_h - n_s} v_r + \frac{n_s}{p_h - n_s} v_s = \frac{p_h v_r - n_s v_s}{p_h - n_s} \tag{5}$$

C. BASIC PARAMETERS AND INITIAL DESIGN

The purpose of the designed LMG is to employ the direct-drive wave power generation system. In order to obtain the stable performance in the marine environment, the number of the field modulation segments is set to 13. In the wave power generation system, it is necessary to perform the sealing treatment procedure and protect the energy convertor against the corrosion. Moreover, the air gap length should be larger than 1 mm. In order to ensure the mechanical strength of the system, the mover yoke thickness is more than 10 mm. On the other hand, the outer diameter is initially determined by the power level of the system. Therefore, a further optimization of the LMG is performed prior to the prototype production.

III. LINEAR MAGNETIC GEAR DESIGN AND OPTIMIZATION

Considering the double air-gap structure of the LMG, conventional methods, including analytical ones are not applicable to optimize the LMG. Reference 13 analyzed the electromagnetic properties of LMG, however, there is no mention of the optimization methods. In other words, conventional methods are difficult to perform, while they are not accurate for this problem. Therefore, the present work proposes the PSO-FEM method, which is a combination of the PSO and FEM methods. The advantageous of the proposed method over the conventional methods is its high accuracy in the machine optimization [14]. However, the computational expenses of the method significantly increase as the optimization parameters increase. In fact, it is not reasonable to perform the PSO-FEM scheme to optimize all parameters. Therefore, in order to decrease the computational expenses of the proposed method, a sensitivity analysis is performed on the geometric parameters. Parameters are categorized into sensitive and non-sensitive ones in this regard.

Due to the axisymmetric structure of the LMG, a two-dimensional finite-element analysis model is established to analyze the electromagnetic characteristics of the LMG, and the balloon boundary condition is considered in the process of analysis. The optimization flowchart in Fig. 4 indicates that the PSO-FEM method is applied only to sensitive parameters.

A. OPTIMIZATION MODEL

The LMG is employed to improve the performance of the direct-drive wave power take-off system. The objective function is selected in accordance with the system optimization requirements, as the following:

$$O(x_i) = \max\{\omega_1 F_{1\max}(x_i) + \omega_2 F_{2\max}(x_i)\} \tag{6}$$

where F_{1max} and F_{2max} are the maximum thrust force of the mover1 and mover2, respectively. Moreover, w_1 and w_2 are weight coefficients and adjust the impact of each force on the objective function. Since the force transmission is more important in the direct-drive wave power take-off system, w_1 and w_2 are set to 0.5. Furthermore, the optimization parameter vector$(\boldsymbol{x})_\mathbf{i}()$ is defined as the following:

$$\begin{aligned} x_i &= [x_1\ x_2\ x_3 x_4\ x_5\ x_6\ x_7\ x_8 x_9\ x_{10}\ x_{11}\ x_{12}\ x_{13}\ x_{14}]^T \\ &= [H_y\ H_{w1}\ W_{w1}\ H_{pm1}\ W_{pm1}\ W_{too1}\ gW_{fm} \\ &\quad H_{fm}\ H_{pm2}\ W_{pm2}\ W_{too2}\ H_{w2}\ W_{w2}]^T \end{aligned} \tag{7}$$

In order to ensure the system reliability and prevent geometrical inconsistencies, parameters are limited in

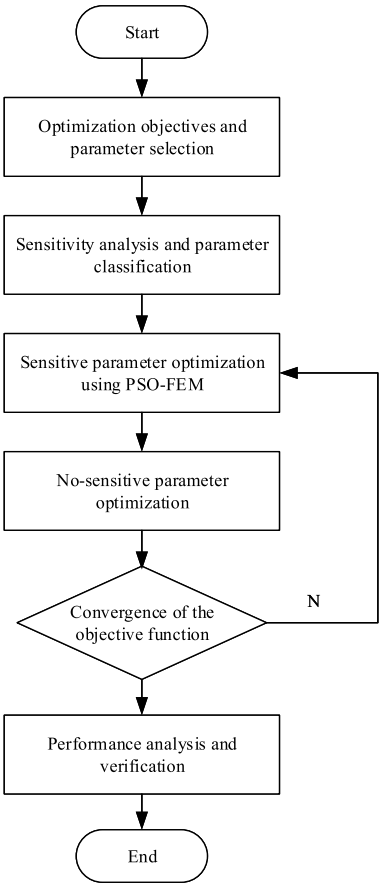

FIGURE 4. Flowchart of the optimization.

accordance with equation (8):

$$\begin{cases} 10\ mm \le H_y \le 25\ mm \\ 3\ mm \le H_{w1} \le 5\ mm \\ 2\ mm \le W_{w1} \le 4\ mm \\ 10\ mm \le L_{pm1} \le 15\ mm \\ 3\ mm \le W_{pm1} \le 6\ mm \\ 3\ mm \le W_{too1} \le 6\ mm \\ 1\ mm \le g \le 2\ mm \\ 3\ mm \le W_{fm} \le 6\ mm \\ 5\ mm \le L_{fm} \le 10\ mm \\ 10\ mm \le L_{pm2} \le 15\ mm \\ 3\ mm \le W_{pm2} \le 6\ mm \\ 3\ mm \le W_{too2} \le 6\ mm \\ 1\ mm \le H_{w2} \le 2\ mm \\ 2\ mm \le W_{w2} \le 4\ mm \end{cases} \tag{8}$$

B. SENSITIVITY ANALYSIS

Based on the section III, the sensitivity analysis is performed to decrease the computational expenses. Therefore, the sensitivity index is defined as at the first stage:

$$S(x_j) = \frac{x_{jo}}{O(x_o)} \cdot \left.\frac{\partial O}{\partial x_j}\right|_{x_i = x_o} = \frac{\Delta O / O(x_o)}{\Delta x_j / x_{jo}} \tag{9}$$

TABLE 1. Preliminary parameters of the LMG.

Symbol	Item	Value
H_y	Mover thickness (mm)	12
H_{w1}	Magnetizing winding1 height (mm)	4
W_{w1}	Magnetizing winding1 width (mm)	5
H_{pm1}	PM1 height (mm)	6
W_{pm1}	PM1 width (mm)	10
W_{too1}	Tooth1 width (mm)	3
g	Air-gap length (mm)	1
W_{fm}	Field modulation segment width (mm)	3
H_{fm}	Field modulation segment height (mm)	6
H_{pm2}	PM2 height (mm)	6
W_{pm2}	PM2 width (mm)	4.6
W_{too2}	Tooth2 width (mm)	1.18
H_{w2}	Magnetizing winding1 height (mm)	4
W_{w2}	Magnetizing winding1 width (mm)	2.3

TABLE 2. Sensitivity indices for each parameter.

Design Parameter	Sensitivity $S_{o\psi}(\%)$
H_y	4.28
H_{w1}	3.45
W_{w1}	3.46
H_{pm1}	18.27
W_{pm1}	31.15
W_{too1}	16.72
g	28.34
W_{fm}	5.56
H_{fm}	26.45
H_{pm2}	18.34
W_{pm2}	32.34
W_{too2}	18.34
H_{w2}	3.45
W_{w2}	3.67

where x_j and $\boldsymbol{x}_0$ denote the parameter to be measured and the initial design of the LMG, respectively. Table 1 illustrates the preliminary parameters of the LMG. It should be indicated that parameters are set in accordance with the results from the FEM analysis and the experiment.

Equation (6) indicates that the objective function consists of two separate terms. Therefore, the sensitivity function S_O can be written as:

$$S_O = k_1 \left|S_{F1\max}(x_i)\right| + k_2 \left|S_{F2\max}(x_i)\right| \tag{10}$$

Combining equations (8) and (10), sensitivity parameters are calculated and the results are shown in Table 2.

Basing on the sensitivity indices for each parameter above the Table 3, the design parameters are divided into two levels by reference 14, as the following:

$$\begin{cases} Non\text{-}sensitive\ parameters : S_O < 10\% \\ sensitive\ parameters : S_O \ge 10\% \end{cases} \tag{11}$$

Sensitive parameters have higher impacts on the performance of the LMG, in comparison to those from non-sensitive parameters. Based on section III, the PSO-FEM method is applied only to sensitive parameters so that the optimization

TABLE 3. Optimal values for sensitive parameters.

Design Parameter	Optimal Value
H_{pm1}	5.68 mm
W_{pm1}	9.72 mm
W_{too1}	3.24 mm
g	1 mm
H_{fm}	5.72 mm
H_{pm2}	6.12 mm
W_{pm2}	4.48 mm
W_{too2}	1.08 mm

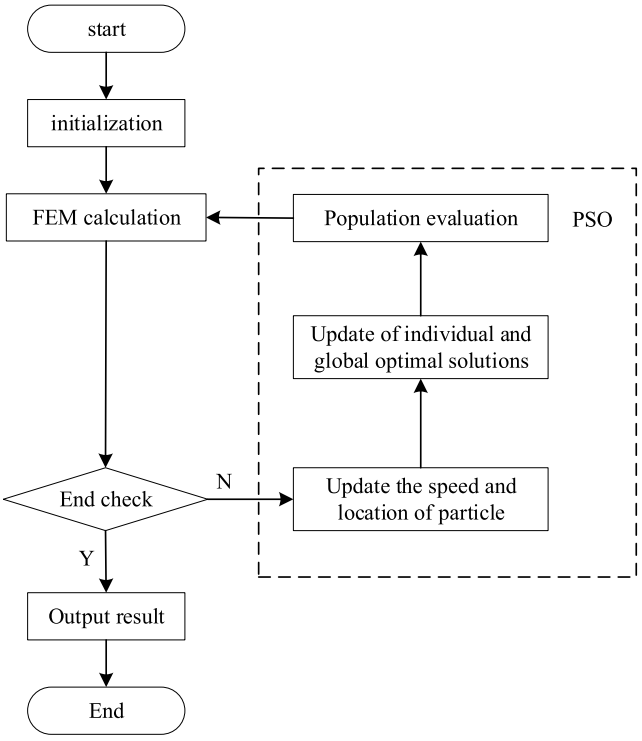

FIGURE 5. Flowchart of the PSO-FEM methodology.

parameters are significantly reduced and calculation speed remarkably improves.

C. OPTIMIZING SENSITIVE PARAMETERS

Fig. 5 illustrates the flowchart of the proposed PSO-FEM method. It should be indicated that the PSO method is employed to optimize functions, which are not easily described in the analytical way [15]. Fig. 6 illustrates the flowchart of the PSO method. Inequality (12) is checked at each iteration to determine the end point of the PSO scheme.

$$\left|F_{gbest} - F_i\right| < \varepsilon \tag{12}$$

where F_{gbest} is the best fitness value, F_i is the value of ith output value.

The FEM analysis is performed on the experiment results to calculate the population. In order to have a reasonable accuracy and computational expense, the population size is set as 30. Particles are randomly distributed to initiate the simulation. Each particle is defined with its location and velocity.

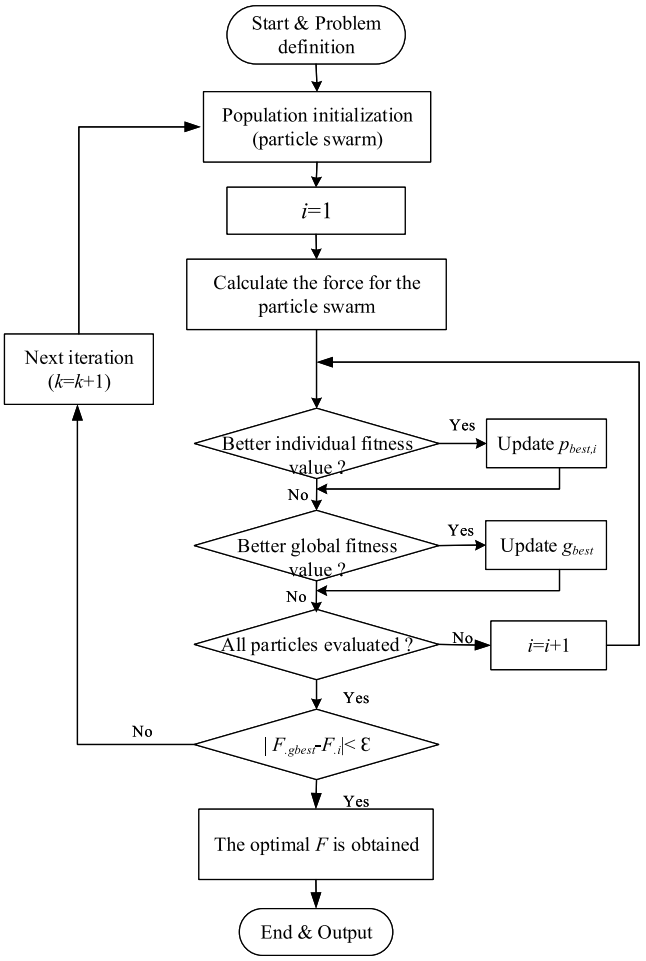

FIGURE 6. Flowchart for the PSO method.

Particle velocity and location at t = each iteration is updated through the following equations:

$$v_i^{k+1} = \omega v_i^k + c_1(P_{best_i}^k - x_i^k)rand_1^k + c_2(G_{best_i}^k - x_i^k)rand_2^k \tag{13}$$

$$x_i^{k+1} = x_i^k + v_i^{k+1} \tag{14}$$

where v_i^k and w denote the i^{th} particle velocity in the k^{th} iteration and the inertia weight with the variation range of [0, 1], respectively. Moreover, c_1 and c_2 are the learning factors and they are normally set to $c_1 = c_2 = 2$. x_i^k, $P_{best_i}^k$ and $G_{best_i}^k$ denote the location of the i$^{\text{th}}$ particle in the k^{th} iteration, the best location of the i^{th} particle based on particle experience and the best particle location based on the overall swarm's experience, respectively. $rand_1^k$ and $rand_2^k$ are two random numbers varying from 0 to 1.

Table 3 illustrates optimal values for sensitive parameters.

IV. FEM SIMULATION

According to results of the performed optimization, a two-dimensional model of the LMG with adjustable gear ratios is established. Since it is not reasonable to set the gear ratio

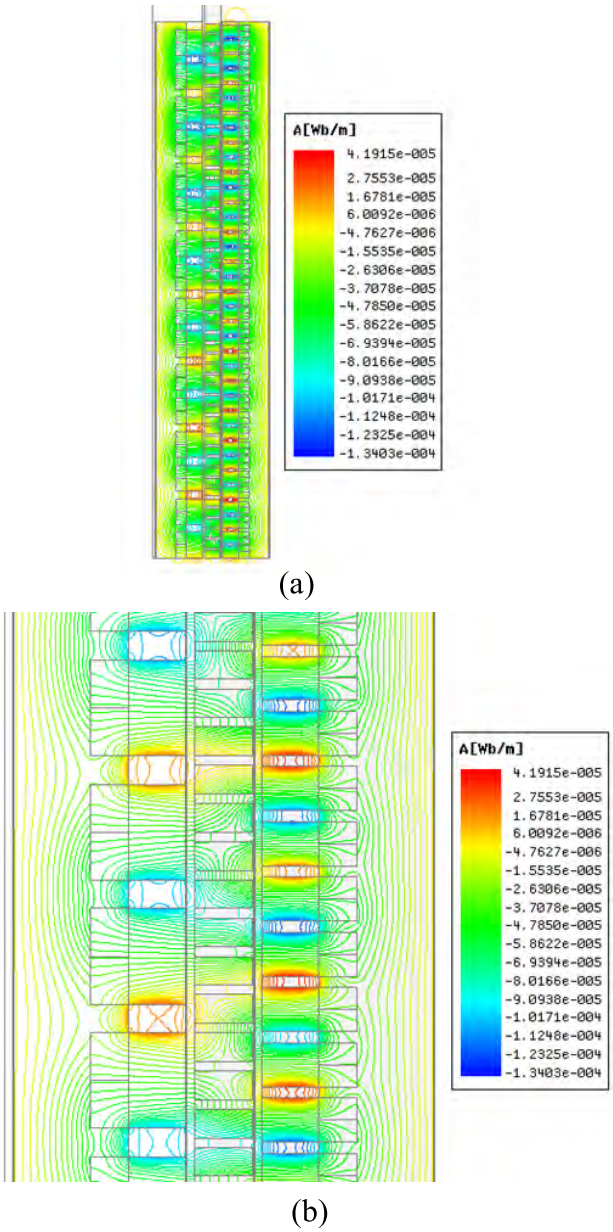

FIGURE 7. Flux-line distribution of the optimal LMG. (a) Overall distribution. (b) Local distribution.

of the LMG to 1, therefore, the present work focuses on gear ratios higher than 1. In order to analyze the electromagnetic characteristics of the LMG conveniently, the number of PM pole pairs in the high-speed mover n_2 is set 4, the number of PM pole pairs in the low-speed mover n_1 is set 4, and the number of ferromagnetic modulator poles Q is set 13. Moreover, the gear ratio and the current of the magnetizing winding are set to 2.25 and 10 A, respectively. Fig.6 illustrates the flux-line distribution of the optimal LMG, where Figs. 7(a) and 7(b) show the overall and local distributions, respectively.

When the gear ratio is set to 9:4, Figs. 8 and 9 illustrate waveforms of the air gap flux density near the mover1 and mover2, respectively. It is observed that there exist 4 and

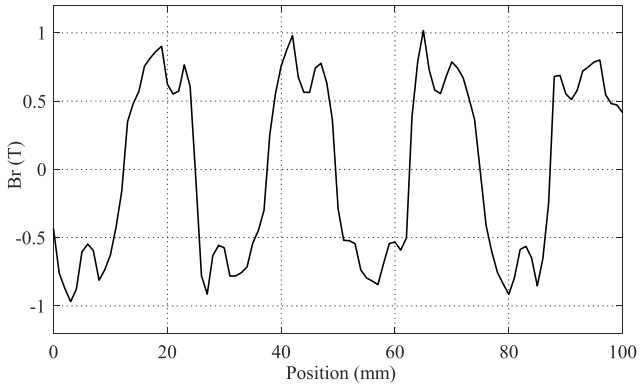

FIGURE 8. Flux density of the air-gap near the mover1, when the gear ratio is set to 9:4.

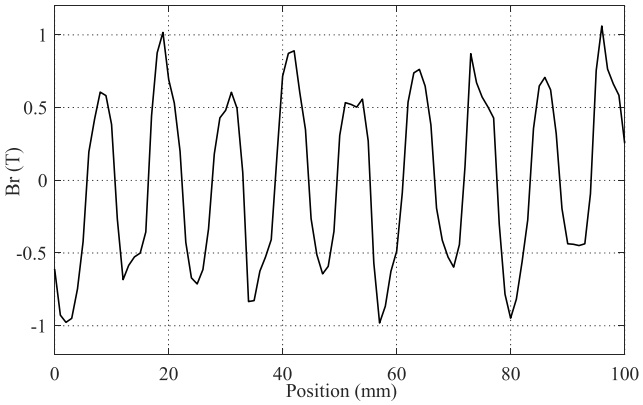

FIGURE 9. Flux density of the air-gap near the mover2, when the gear ratio is set to 9:4.

9 pole-pairs of air-gap magnetic fields near the mover1 and mover2, respectively.

The experiment area is located in eastern China and according to the survey, wave speeds vary from 0.4 m/s to 1.5 m/s. In the course of the study, the speed of low-speed mover is constant and it is set to 0.4 m/s for the convenience of the linear magnetic gear study. Moreover, based on the analysis discussed above, the speed of high-speed mover is 1.3 m/s. Fig. 10 shows the force characteristic on the mover1 and mover2. It indicates that the average amplitude force of mover2 is 1.39 kN, while that for the mover1 is 0.43 kN. Therefore, the output forces of the low- and high-speed movers can be adjusted by changing the magnetic gear modulation characteristics so that the conversion efficiency of the direct drive wave power generation system can be improved.

V. APPLICATION IN WAVE POWER TAKE-OFF SYSTEM

The direct-driven wave power take-off systems with no intermediate energy conversion devices have the advantage of high efficiency and high reliability [16]–[18].

For investigation of the direct-drive wave power take-off system, the following assumptions are considered in the present study:

a) The buoy motion is only in the vertical direction.
b) The buoy radius is small, compared with the wavelength.

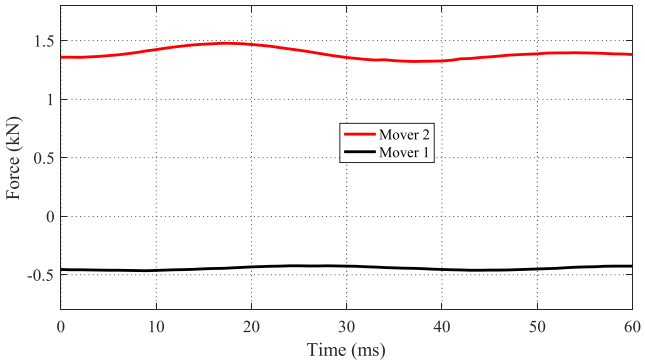

FIGURE 10. Force transmission distribution along time, when the gear ratio is set to 9:4.

c) The connecting rod between the buoy and the generator translator is rigid.
d) The linear potential theory is employed in the calculations [19].

Equation (15) describes the motion of the wave power take-off system from the mathematical point of view:

$$(m + m_r(\omega))\ddot{x}(t) + R_r(\omega)\dot{x}(t) + Sx(t) = F_e + F_{PTO} + F_s \tag{15}$$

where m is the buoy mass, including the mass of translator of the linear generator and the mass of the lower-speed mover of the LMG. Moreover, m_r, $x(t)$, R_r and S denote the added mass, buoy position, radiation damping and the hydrostatic stiffness, respectively. On the other hand, F_e, F_{PTO} and F_s are the excitation force, wave power take-off (PTO) force, including losses and the spring force, respectively.

It is found that for incident waves with the frequency equal to the natural frequency of the converter, the resonance takes place. Studies show that the wave power take-off system harvests the maximum amount of energy from waves. The system resonates, when the reactance of the system reaches to zero. This is mathematically written as:

$$\omega_0(m + m_r) - \frac{S}{\omega_0} = 0 \tag{16}$$

Equation (16) indicates that the resonance takes place, when the potential and the kinetic energy storage of the system are of the same size [20]. The resonance period of the system can be calculated as:

$$T_0 = \frac{2\pi}{\omega_0} = 2\pi\sqrt{(m + m_r)/S} \tag{17}$$

It should be indicated that the movement velocity of the linear generator, which is connected to the LMG, is not constant. On the other hand, mover1 and mover2 have motions in the opposite directions. In order to calculate the linear generator velocity and the spring displacement, their initial values are updated with a corrective coefficient, called G_r. Equations (18) and (19) shows expressions to calculate the spring force F_s and the generator force F_{PTO} at each time step.

$$F_s(x, t) = -k_s[-G_r x(t)] = k_s G_r x(t) \tag{18}$$

TABLE 4. Key parameters of wave power take-off system.

Parameter	Value
Buoy radius	0.5 m
Buoy mass	10 kg
Translator mass	40 kg
Added mass	30 kg
Spring constant	0.5 kN/m
Generator damping coefficient	0.4kNs/m
Remnant flux density of the AlCiO PM	1.05 T

$$F_{PTO}(x, t) = -k_g[-G_r\dot{x}(t)] = k_g G_r\dot{x}(t) \tag{19}$$

where k_s and k_g denote the spring constant and the damping coefficient of the generator, respectively.

According to the above analysis, the natural period of the wave energy converter is re-written as:

$$T_0 = 2\pi\sqrt{\frac{m + m_r}{\rho g\pi a^2 - k_s G_r}} \tag{20}$$

where ρ, g and a denote the water density, acceleration of the gravity and the buoy radii, respectively.

Equation (20) indicates that the natural frequency of the wave energy converter depends on different parameters, including the mass and ratio of the gear. In other words, the natural frequency of the system can be adjusted by setting the system configuration. The optimum trajectory for a single-mode absorber can be determined as a function of relative phase and amplitude between the wave and the buoy oscillation. The velocity phase should agree with the one for the excitation force. Then, the amplitude is set to obtain the best interference with the incident wave.

Based on the principle of small amplitude waves, the period of incident waves is calculated as the following:

$$T = \sqrt{\frac{2\pi L}{g} c * th(kd)} \tag{21}$$

$$k = \frac{2\pi}{L} \tag{22}$$

$$c = \frac{gT}{2\pi} th(kd) \tag{23}$$

where L and d are the wavelength and seawater depth, respectively. In order to investigate the performances of the proposed method, the system response to a wave with variable energy period is studied. Mover1 is connected to the buoy, while the mover2 is mechanically coupled to the PMLG. Table 4 shows the characteristics of the wave power take-off system.

Table 5 shows the variation of the resonance frequency with gear ratios. It is observed that the oscillation frequency of the wave power take-off system varies with the change of the LMG ratio. It indicates that the maximum power tracking can be obtained by adjusting the transmission ratio of the LMG.

TABLE 5. Resonance frequency varies with gear ratios.

Period (s)	*Resonance frequency (rad/s)*	G_r
0.83	*7.55*	*1*
0.94	*6.68*	*1.2*
1.34	*4.67*	*1.5*
1.50	*4.20*	*1.8*
1.56	*4.02*	*2.25*

TABLE 6. Parameters of the PMLG.

parameters	*Item*	*Value*
τ_s	*pole pitch*	*21.5mm*
τ_{mr}	*length of radial permanent magnet*	*14.5 mm*
τ_{mz}	*length of axial permanent magnet*	*7 mm*
τ_c	*slot pitch*	*19.5mm*
ω_s	*width of slot*	*10.5 mm*
R_o	*outer diameter*	*54.5 mm*
R_i	*inner diameter*	*10 mm*
H_b	*thickness of the back iron*	*13.5 mm*
H_{PM}	*thickness of the permanent magnet*	*3 mm*
g	*air-gap*	*3 mm*
W_{te}	*width of edge end tooth*	*9 mm*
ω_n	*width of rabbet*	*4 mm*
H_y	*thickness of the yoke*	*3 mm*
N	*number of turns*	*60*

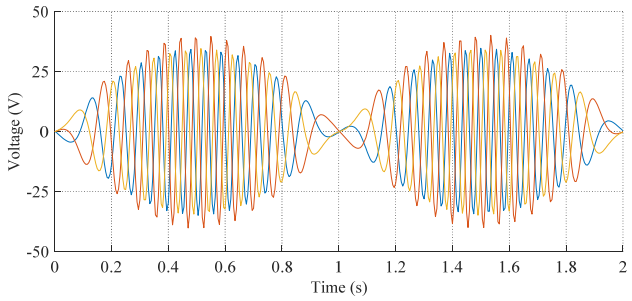

FIGURE 11. Distribution of the output voltage at $G_r = 2$.

Table 6 shows parameters of the PMLG, which are connected to the high-speed mover of the LMG. Liu *et al.* [21]. discussed the specific design of the LMG in details.

In order to perform the analysis, the wave velocity is assumed to be in a sine form as the following:

$v = 0.4*\sin(\pi t)$.

Fig. 11 shows the distribution of the output voltage for $G_r = 2$. Moreover, Fig. 12 illustrates the instantaneous power distribution, when the load is set to $R = 30\ \Omega$ and G_r is equal to 1 and 2. It is observed that, when $G_r = 2$ the instantaneous power value is significantly larger than that for $G_r = 1$. It is found that the maximum and minimum multiples are 5.38 and 2.55, respectively.

The experimental site is located in Zhoushan City, Zhejiang Province, China. In this island, the site is affected by the low wind and terrain and the coastal waves are relatively stable. Wave periods are variable from 1 to 4 seconds and wave heights vary from 0.15 m to 0.5 m. Variables of the AC and DC sides are probed and transmitted to the remote central PC via the GPRS communication system. Fig. 13 shows the direct-drive take-off system and its primary parts, including

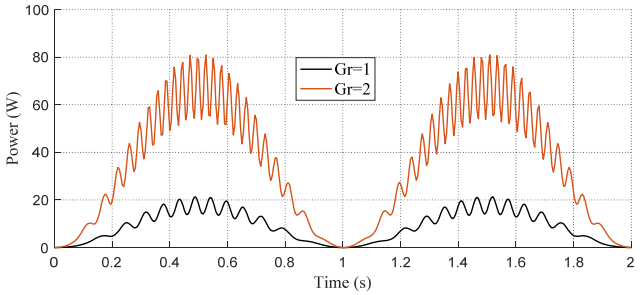

FIGURE 12. Distribution of the instantaneous power at $G_r = 2$.

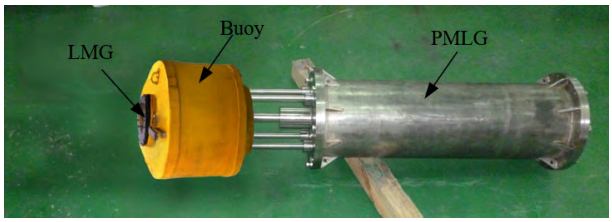

FIGURE 13. Configuration of the direct-drive wave power take-off system.

FIGURE 14. Experiment device in the real oceanic environment.

the buoy, PMLG and the LMG. It illustrates connections of the low-speed and high-speed movers to the buoy and PMLG, respectively. When the wave comes, the buoy follows the wave motion and oscillates up and down. The velocity of the PMLG increases through the magnetic field modulation of the LMG. Therefore, the system extracts more wave energy and the overall efficiency increases. Fig. 14 shows the experiment device in the real oceanic environment. On the day of the experiment, in clear weather, sunny, which was fit for the testing environment. Fig. 15 shows the distribution of the instantaneous output voltage. It is observed that the wave energy is successfully harvested and the electrical energy is obtained. The maximum voltage values of the phase A, B, and C are 47.6 V, 55.3 V, and 47.8 V, respectively. The voltage value of B-phase is higher than the other two phase which is caused by the armature reaction of the PMLG. Fig. 16 shows the instantaneous and average power, obtained from the experimental device and simulation. The experiment values of maximum instantaneous and average power are

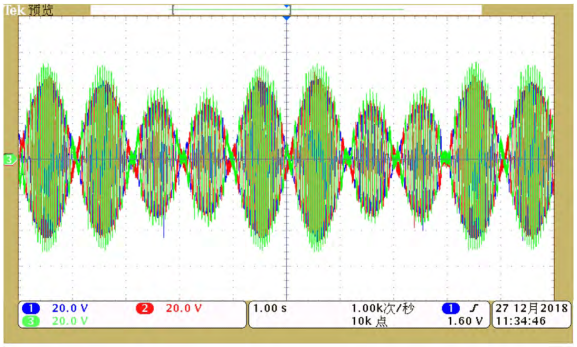

FIGURE 15. Distribution of the instantaneous output voltage.

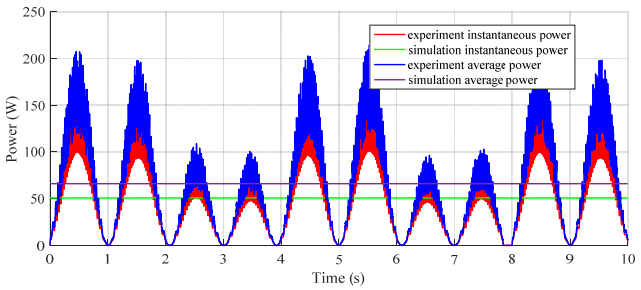

FIGURE 16. Distribution of the instantaneous and average output power.

153. 4 W and 50.8 W, respectively. The simulation values of maximum instantaneous and average are slightly bigger than the experiment, and the values are 214.7 W and 66.1 W, respectively. The reason is that some factors are ignored such as friction and eddy current loss during the simulation. It indicates that 50.8 W of electrical energy is obtained on the average during the experiment.

VI. CONCLUSION

A novel method for optimal design of linear magnetic gears with arbitrary gear ratios is introduced in the present study. In order to reduce computational expenses of the optimization, design parameters are categorized into sensitive and non-sensitive parameters. Then, the PSO-FEM method is employed to optimize the sensitive ones. Using PSO-FEM optimization method, its optimization time decreases from 8 h 32 m to 2 h 18 m (CPU is Intel(R) Core(TM) i7-8550U, frequency is 1.80 GHz, RAM is 8 GB). Moreover, the computational model for the direct-drive wave power take-off system is established and the correlation between the buoy and the incident wave frequency is analyzed. Since adjustable gear ratios are used in the proposed scheme, the natural frequency of the wave energy converter can be set in accordance with the incident wave frequency. Therefore, the proposed scheme can operate in the resonance condition with waves for a wide range of wave frequencies so that the maximum electrical power may be harvested. The carried-out experiment proves that the direct-drive power take-off system, which is composed of the LMG and PMLG, may be an effective method to obtain the electrical energy from the renewable oceanic wave energy.

REFERENCES

[1] A. Elhanafi and J. K. Chan, "Experimental and numerical investigation on wave height and power take–off damping effects on the hydrodynamic performance of an offshore–stationary OWC wave energy converter," *Renew. Energy*, vol. 125, pp. 518–528, Sep. 2018.

[2] F. R. Torres, P. R. F. Teixeira, and E. Didier, "A methodology to determine the optimal size of a wells turbine in an oscillating water column device by using coupled hydro-aerodynamic models," *Renew. Energy*, vol. 121, pp. 9–18, Jun. 2018.

[3] A. Çelik and A. Altunkaynak, "Experimental and analytical investigation on chamber water surface fluctuations and motion behaviours of water column type wave energy converter," *Ocean Eng.*, vol. 150, pp. 209–220, Feb. 2018.

[4] S. L. P. Iahnke, M. N. Gomes, L. A. Isoldi, and L. A. O. Rocha, "Energy from the sea: Computational modeling of an overtopping device," in *Proc. 3rd Southern Conf. Comput. Modeling*, Nov. 2009, pp. 94–99.

[5] J. C. Martins, M. M. Goulart, M. das N. Gomes, J. A. Souza, L. A. O. Rocha, L. A. Isoldi, and E. D. Dos Santos, "Geometric evaluation of the main operational principle of an overtopping wave energy converter by means of constructal design," *Renew. Energy*, vol. 118, pp. 727–741, Apr. 2018.

[6] D. Elwood, A. Schacher, K. Rhinefrank, J. Prudell, S. Yim, E. Amon, T. Brekken, and A. von Jouanne, "Numerical modelling and ocean testing of a direct-drive wave energy device utilizing a permanent magnet linear generator for power take-off," in *Proc. 28th Int. Conf. Ocean Offshore Arctic Eng.*, Honolulu, HI, USA, 2009, pp. 817–824.

[7] D. Elwood, S. C. Yim, J. Prudell, C. Stillinger, A. von Jouanne, T. Brekken, A. Brown, and R. Paasch, "Design, construction, and ocean testing of a taut-moored dual-body wave energy converter with a linear generator power take-off," *Renew. Energy*, vol. 35, no. 2, pp. 348–354, Feb. 2010.

[8] J. Prudell, M. Stoddard, E. Amon, T. K. A. Brekken, and A. von Jouanne, "A permanent-magnet tubular linear generator for ocean wave energy conversion," *IEEE Trans. Ind. Appl.*, vol. 46, no. 6, pp. 2392–2400, Nov./Dec. 2010.

[9] P. Tokat and T. Thiringer, "Sizing of IPM generator for a single point absorber type wave energy converter," *IEEE Trans. Energy Convers.*, vol. 33, no. 1, pp. 10–19, Mar. 2018.

[10] M. I. Marei, M. Mokhtar, and A. A. El-Sattar, "MPPT strategy based on speed control for aWS-based wave energy conversion system," *Renew. Energy*, vol. 83, pp. 305–317, Nov. 2015.

[11] F. Wu, P. Ju, X.-P. Zhang. C. Qin, G. J. Peng, H. Huang, and J. Fang, "Modeling, control strategy, and power conditioning for direct-drive wave energy conversion to operate with power grid," *Proc. IEEE*, vol. 101, no. 4, pp. 925–941, Apr. 2013.

[12] K. Atallah, S. D. Calverley, and D. Howe, "Design, analysis and realisation of a high-performance magnetic gear," *IEE Proc.-Electr. Power Appl.*, vol. 151, no. 2, pp. 135–143, Mar. 2004.

[13] F. Ningjun, Y. Haitao, H. Minqiang, and C. Jielin, "Performance analysis of a tubular linear magnetic gear," *Trans. China Electrotech. Soc.*, vol. 30, no. 2, pp. 43–49, 2015.

[14] Y. C. Wang, S. Niu, and W. Fu, "Sensitivity analysis and optimal design of a dual mechanical port bidirectional flux-modulated machine," *IEEE Trans. Ind. Electron.*, vol. 65, no. 1, pp. 211–220, Jan. 2018.

[15] J. Kennedy and R. Eberhart, "Particle swarm optimization," in *Proc. IEEE Int. Conf. Neural Netw.*, vol. 4, Nov./Dec. 1995, pp. 1942–1948.

[16] C. Liu, H. Yu, Q. Liu, W. Zhong, and H. Zhu, "Research on a double float system for direct drive wave power conversion," *IET Renew. Power Gener.*, vol. 11, no. 7, pp. 1026–1032, Jun. 2017.

[17] I. Temiz, J. Leijon, B. Ekergård, and C. Boström, "Economic aspects of latching control for a wave energy converter with a direct drive linear generator power take-off," *Renew. Energy*, vol. 128, pp. 57–67, Dec. 2018.

[18] C. Liu, J. Zhang, Y. Xiong, H. Zhu, H. Yu, and L. Huang, "Spatial harmonic analysis on a permanent magnet linear generator with Halbach array for direct-driver wave energy conversion," *Int. J. Numer. Model., Electron. Netw., Devices Fields*, vol. 31, no. 5, p. e2316, Sep./Oct. 2017.

[19] J. Engström, V. Kurupath, J. Isberg, and M. Leijon, "A resonant two body system for a point absorbing wave energy converter with direct-driven linear generator," *J. Appl. Phys.*, vol. 110, no. 12, pp. 275–899, Oct. 2011.

[20] J. Falnes, *Ocean Waves and Oscillating Systems: Linear Interactions Including Wave-Energy Extraction*. Cambridge, U.K.: Cambridge Univ. Press, 2002.
[21] C. Liu, H. Yu, M. Hu, Q. Liu, S. Zhou, and L. Huang, "Research on a permanent magnet tubular linear generator for direct drive wave energy conversion," *IET Renew. Power Gener.*, vol. 8, no. 3, pp. 281–288, Apr. 2014.

CHUNYUAN LIU received the B.E. degree from the Lanzhou University of Technology, China, in 2003, the M.S. degree from the Xi'an University of Science and Technology, China, in 2011, and the Ph.D. degree from Southeast University, China, in 2015. He has been a Teacher with the College of Mechanical and Electrical Engineering, Jiaxing University, China. His current research interests include linear machine and wave energy conversion.

HE ZHU was born in Harbin China, in 1979. He received the B.S. degree in Computer Science and Technology from Harbin Institute, the M.S. degree in Power System and its Automation from Harbin Engineering University, and Ph.D. degree in Electric Machines and Electric Apparatus from the Harbin Institute of Technology, Harbin, China, in 2015. Since 2015,he has been working as a Lecturerwith the College of Mechanical and Electrical Engineering of Jiaxing University. His research interests include electric motor drive and control system.

RUI DONG received the M.S. degree in electrical engineering from the Wuhan University of Technology, China, in 2010. His research interest includes power electronics equipment, drive of PMSM and Linear Motor.

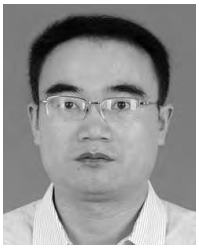

SHIGUI ZHOU received the Ph.D. degree from Southeast University, Nanjing, China, in 2013.He has been with Qufu Normal University, where he is currently an Associate Professor in the School of Engineering. His current research interests include the design, analysis, and control of electrical machines.

LEI HUANG (M'16) received the B.Eng. and M.Eng. degrees from the China University of Petroleum (UPC), Dongying, China, in 2002 and 2008, respectively, and the Ph.D. degree from the Southeast University, Nanjing, China., in 2012, all in electrical engineering.He is currently an Associate Professor in Electrical Engineering with the Southeast University, Nanjing, China. He was a visiting scholar at the University of Sheffield, Sheffield, U.K., from 2017 to 2018. His research interests include linear generators and electromechanical energy conversion to direct-drive wave energy conversion.